

SUPPLEMENTARY INFORMATION

The Structure of SpnF, a Standalone Enzyme that Catalyzes [4+2] Cycloaddition

Christopher D. Fage^{1,*}, Eta A. Isiorho^{1,*}, Yungnan Liu², Drew T. Wagner¹,
Hung-wen Liu^{2,3} & Adrian T. Keatinge-Clay^{1,3}

¹Department of Molecular Biosciences,

The University of Texas at Austin, Austin, TX 78712

²Division of Medicinal Chemistry, College of Pharmacy,

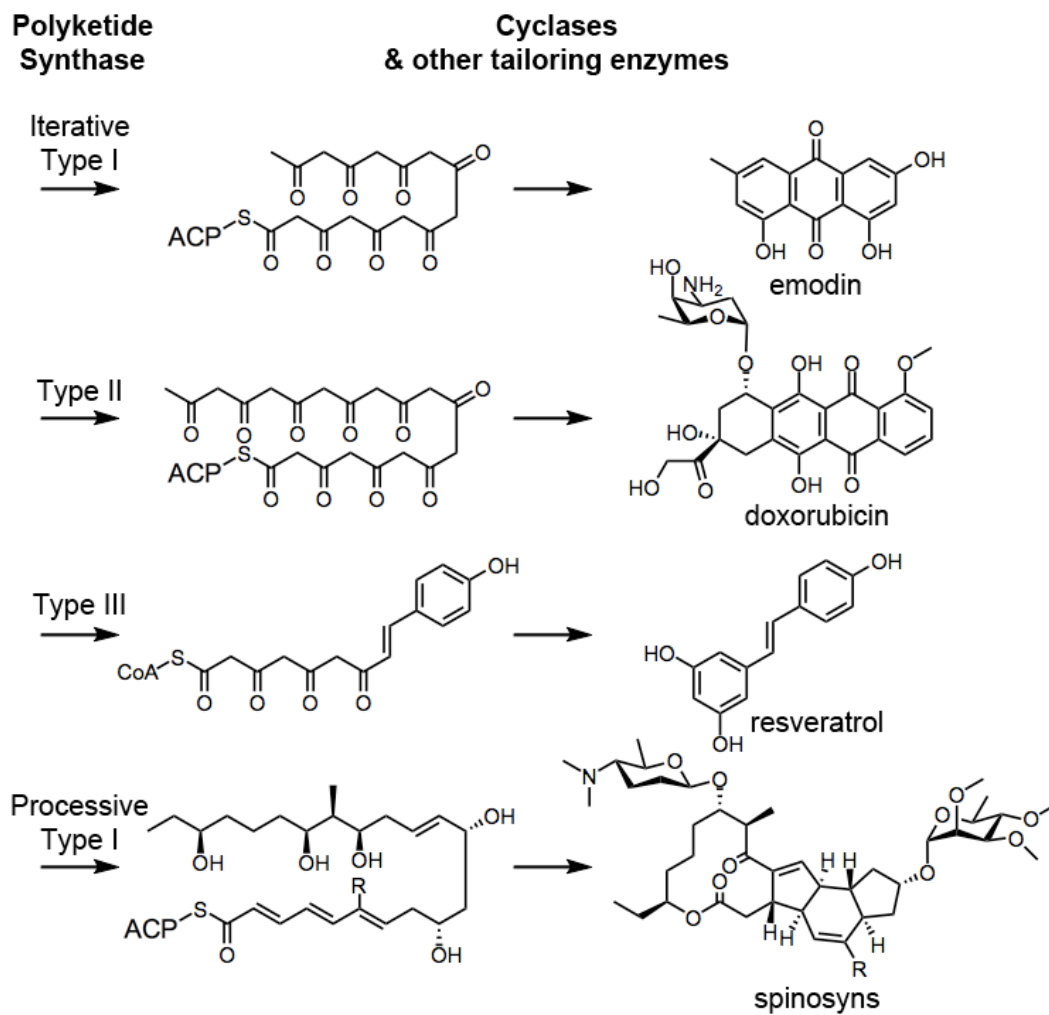
The University of Texas at Austin, Austin, TX 78712

³Department of Chemistry,

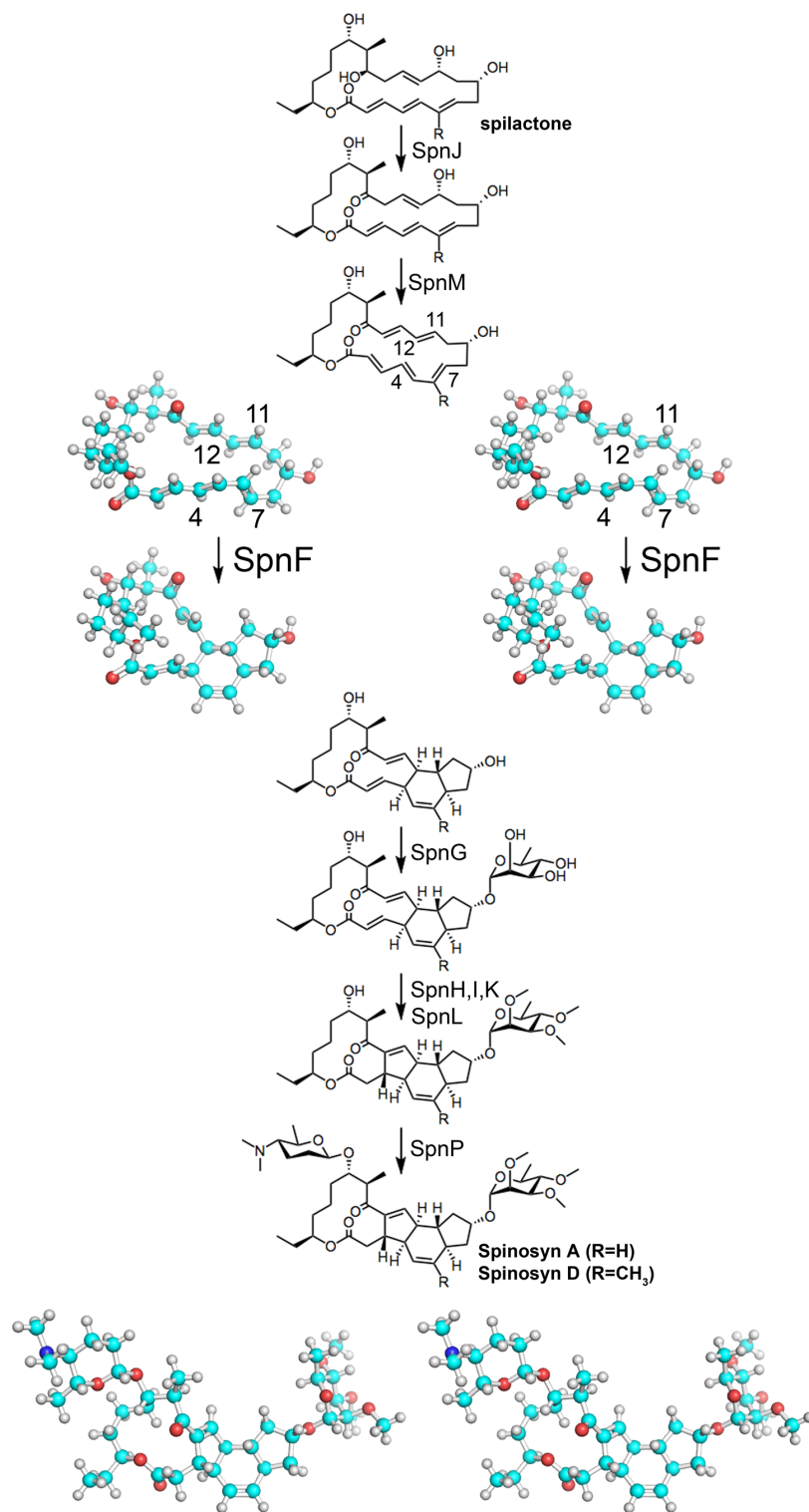
The University of Texas at Austin, Austin, TX 78712

* authors made equal contributions

SUPPLEMENTARY RESULTS



Supplementary Figure 1. Generation of polyketides containing carbocycles. Cyclases that accompany iterative PKSs often mediate the formation of polyketides with carbocyclic rings. The spinosyn biosynthetic pathway is rare in that it contains a processive Type I PKS and generates carbocyclic products.



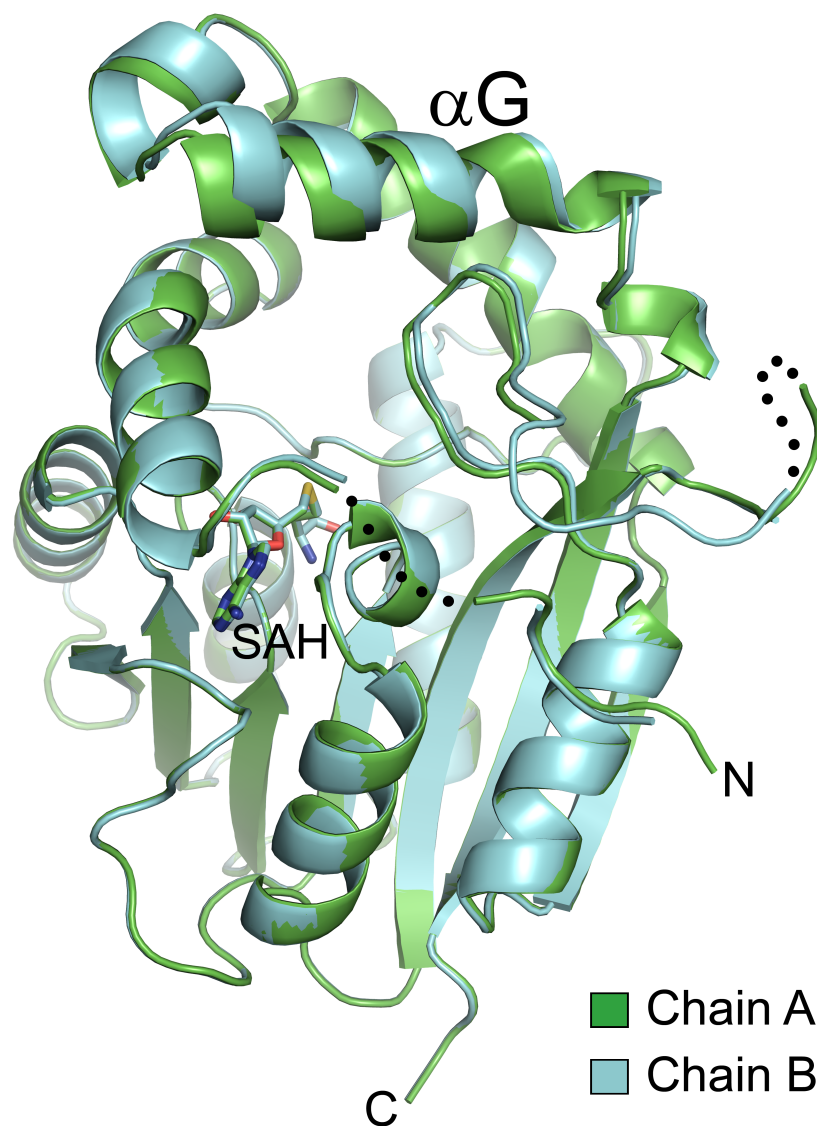
Supplementary Figure 2. A closer look at the spinosyn tailoring reactions. After generation of spilactone by a processive Type I PKS, SpnJ catalyzes oxidation of the C15-hydroxyl group to

a ketone functionality¹. Next, SpnM catalyzes a 1,4-dehydration² yielding a second, π -conjugated system that contains the putative dienophile. SpnF then catalyzes cyclohexene ring formation via [4+2]-cycloaddition between the C11-C12 dienophile and the C4-C7 diene². The tricyclic intermediate is subsequently rhamnosylated at C9 in a glycosylation reaction catalyzed by SpnG^{3,4}, after which the rhamnose moiety is permethylated through the combined activities of the *S*-adenosylmethionine (SAM)-dependent methyltransferases, SpnH, SpnI and SpnK⁵. SpnL facilitates cross-coupling between C3 and C14 to complete the construction of the tetracyclic skeleton². Finally, SpnP transfers forosamine to C17 to generate the biologically-active spinosyns⁶.

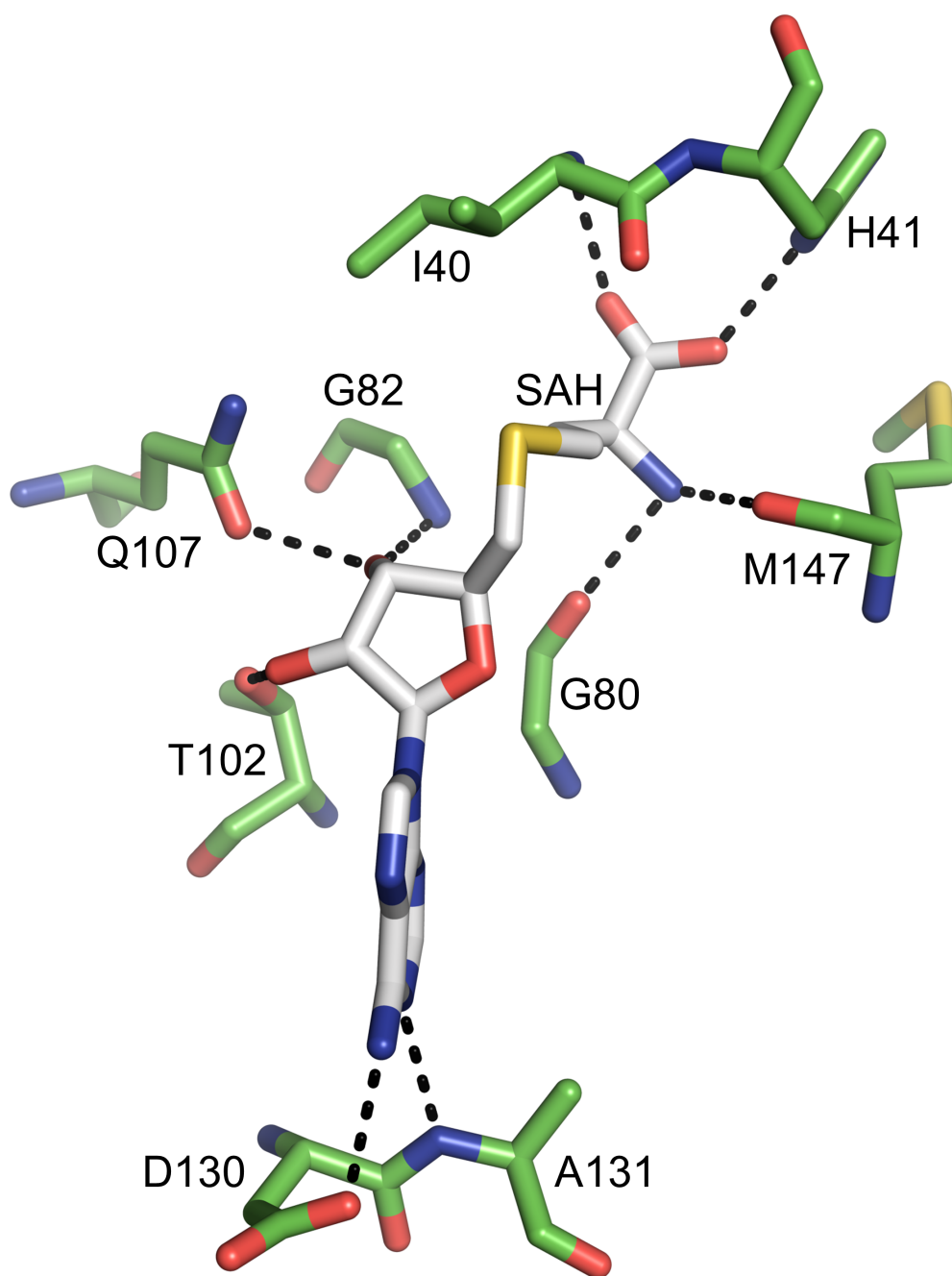
Supplementary Table 1. Data collection and refinement statistics (molecular replacement)

SpnF/SAH	
Data collection	
Space group	
Cell dimensions	
<i>a</i> , <i>b</i> , <i>c</i> (Å)	41.74, 69.35, 83.63
α , β , γ (°)	90, 97.50, 90
Resolution (Å)	82.92-1.50(1.54-1.50)*
<i>R</i> _{sym}	0.112(0.964)
<i>I</i> / σI	9.12(1.56)
Completeness (%)	98.0(97.4)
Redundancy	3.7(3.8)
Refinement	
Resolution (Å)	82.92-1.50(1.52-1.50)
No. reflections	74131(2578)
<i>R</i> _{work} / <i>R</i> _{free}	0.197/0.222(0.288/0.332)
No. atoms	8506
Protein	8158
Ligand/ion	126
Water	222
<i>B</i> -factors (Å ²)	19.73
Protein	20.46
Ligand/ion	14.99
Water	23.73
R.m.s. deviations	
Bond lengths (Å)	0.011
Bond angles (°)	1.37

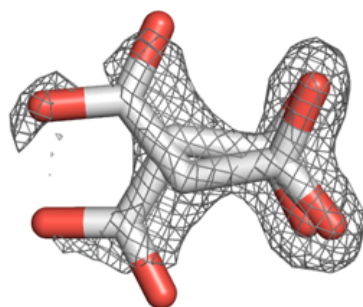
*Highest-resolution shell is shown in parentheses. Data were acquired from a single crystal.



Supplementary Figure 3. Superposed SpnF monomers. Two monomers, chain A (green) and chain B (cyan), were observed in the asymmetric unit. These monomers align well, with 0.165 Å r.m.s.d. over 1357 atoms and 0.131 Å r.m.s.d. over 206 C_{α} atoms. A slight difference in the pitch of helix αG can be seen. Dotted lines indicate regions for which no electron density is observed.

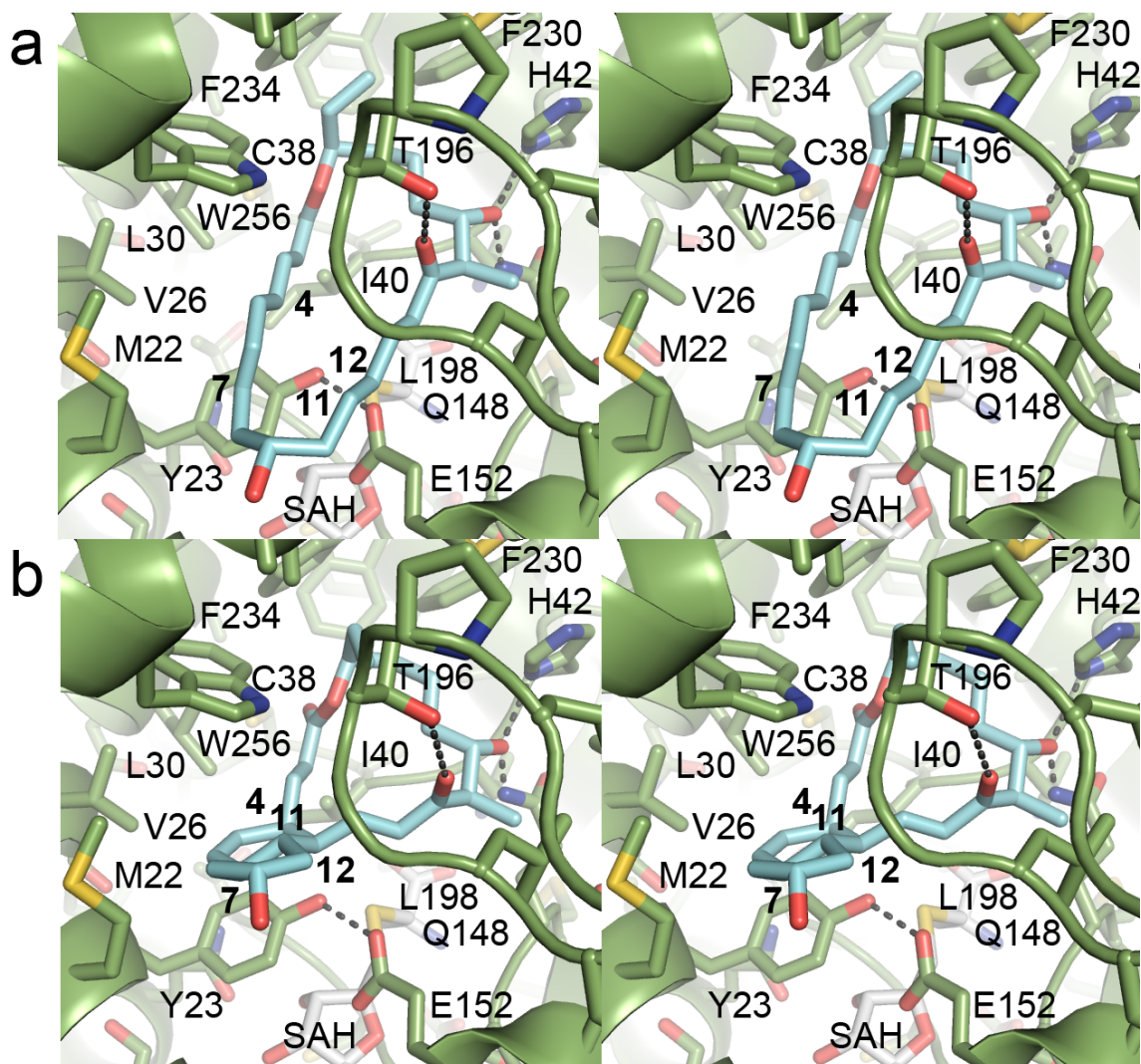


Supplementary Figure 4. Interactions with SAH. All contacts made between SAH and SpnF via hydrogen bonds are illustrated.



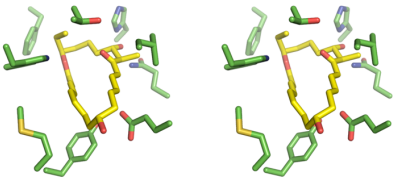
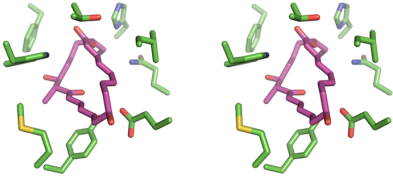
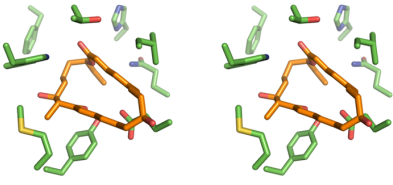
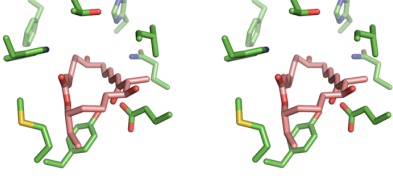
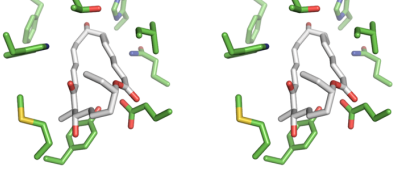
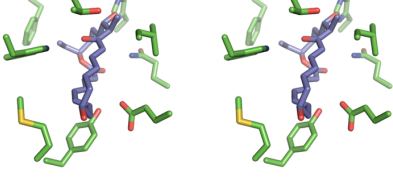
malonate (MLI)

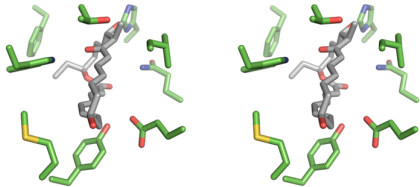
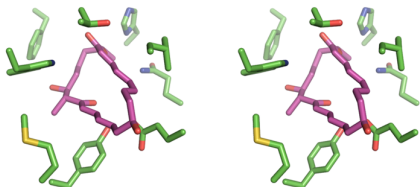
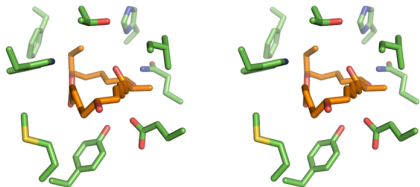
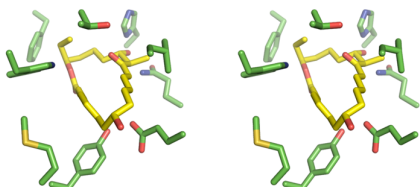
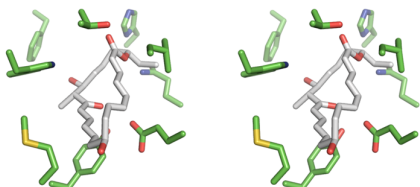
Supplementary Figure 5. Density in the substrate cavity. The electron density maps of each monomer in the asymmetric unit reveal the presence what appears to be malonate in two conformations. Here, the F_o-F_c omit map contoured at 4.0 r.m.s.d. illustrates this electron density.

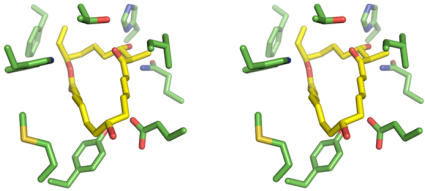
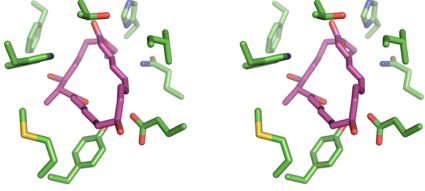
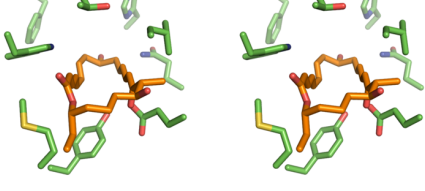
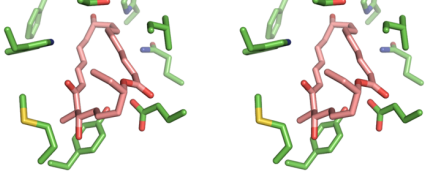


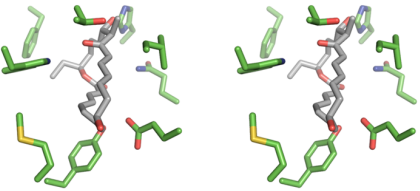
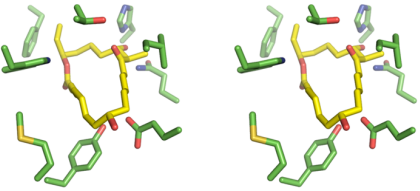
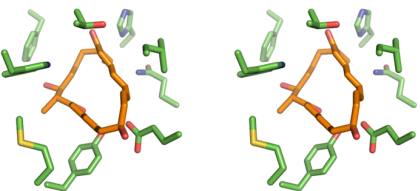
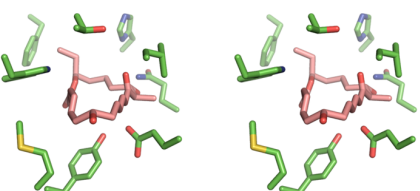
Supplementary Figure 6. Stereodiagrams of computationally-docked SpnF substrate and product. As described in Figure 2b, the majority of contacts are hydrophobic although the C17-OH forms hydrogen bonds with both H42 and Q148. The C11-C12 π -bond may be polarized by T196 through its hydrogen bond to the C15 keto group to react with the C4-C7 diene. SAH does not make contact with either the substrate or product.

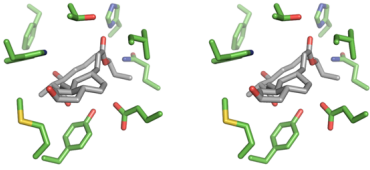
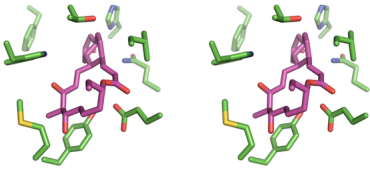
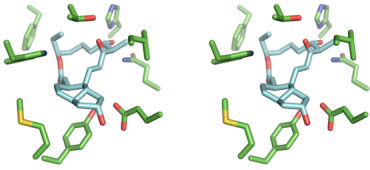
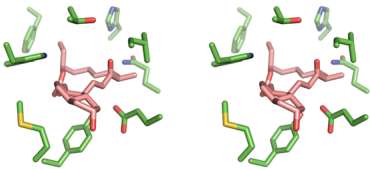
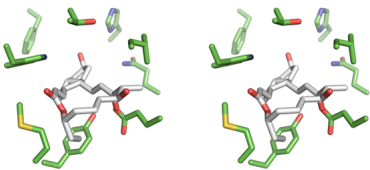
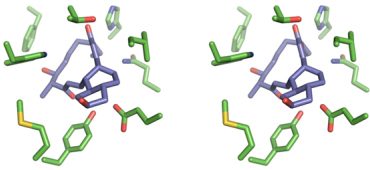
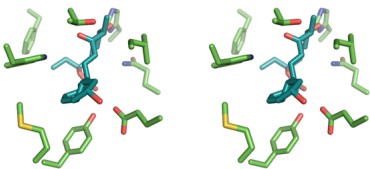
a

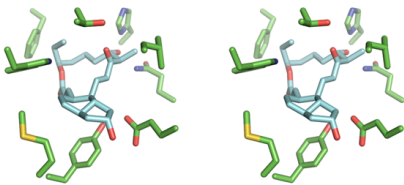
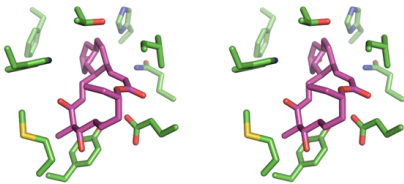
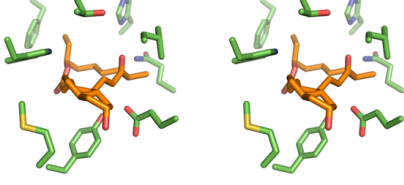
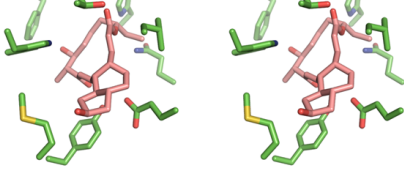
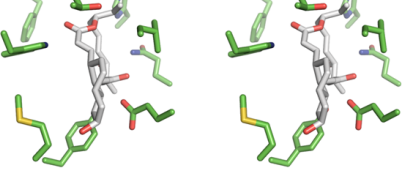
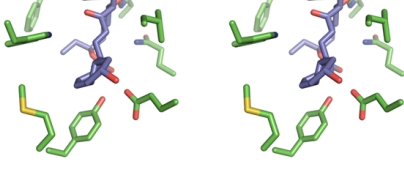
Substrate (UFF), AutoDock Vina		
Mode	Affinity (kcal/mol)	Docked pose
1	-7.5	
2	-7.1	
3	-5.9	
4	-5.3	
5	-5.0	
6	-4.9	

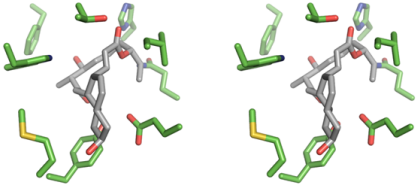
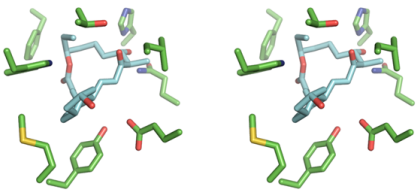
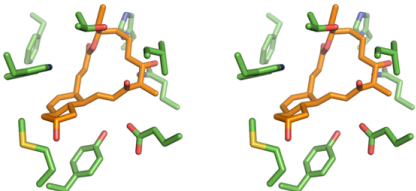
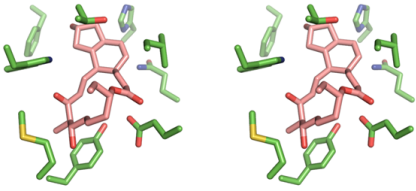
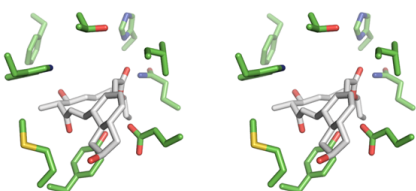
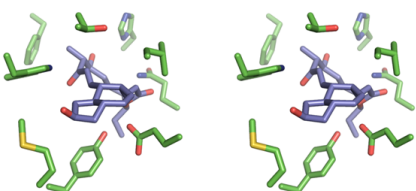
Substrate (UFF), DOCK6.6		
Mode	Grid score	Docked pose
1	-27.5	
2	-25.7	
3	-10.5	
4	-5.4	
5	-1.2	

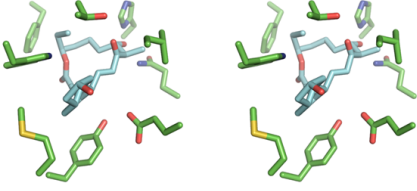
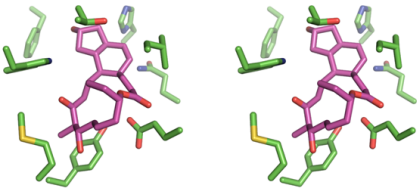
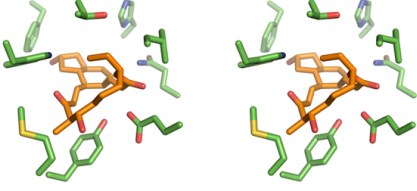
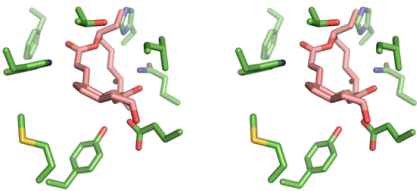
Substrate (MMFF94s), AutoDock Vina		
Mode	Affinity (kcal/mol)	Docked pose
1	-7.6	
2	-5.9	
3	-5.6	
4	-4.6	

Substrate (MMFF94s), DOCK6.6		
Mode	Grid score	Docked pose
1	-18.4	
2	-9.1	
3	-3.7	
4	88.2	

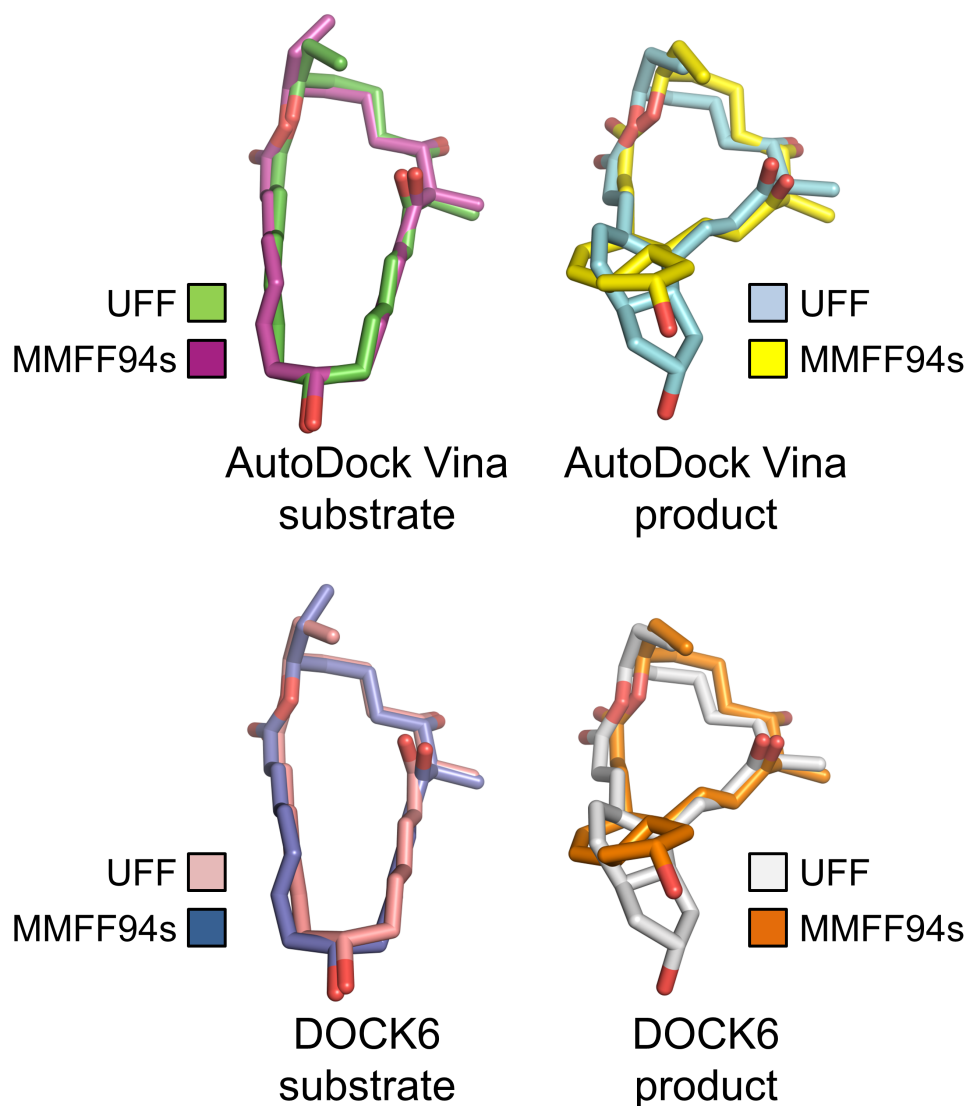
Product (UFF), AutoDock Vina		
Mode	Affinity (kcal/mol)	Docked pose
1	-7.0	
2	-6.6	
3	-6.3	
4	-6.2	
5	-5.7	
6	-4.6	
7	-4.1	

Product (UFF), DOCK6.6		
Mode	Grid score	Docked pose
1	-24.8	
2	-13.7	
3	-12.1	
4	-8.27	
5	3.6	
6	3.7	

Product (MMFF94s), AutoDock Vina		
Mode	Affinity (kcal/mol)	Docked pose
1	-6.0	
2	-5.4	
3	-4.6	
4	-4.5	
5	-3.3	
6	-3.2	

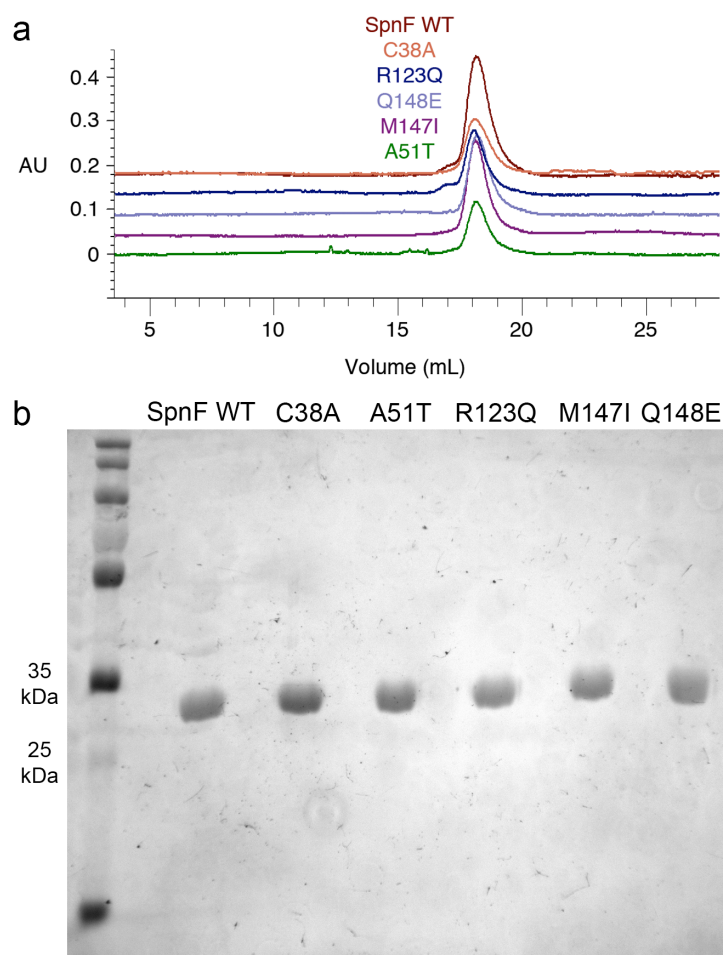
Product (MMFF94s), DOCK6.6		
Mode	Grid score	Docked pose
1	3.0	
2	15.8	
3	58.0	
4	69.3	

b



Supplementary Table 2. Docking output for the SpnF substrate and product. a) Molecules were docked in AutoDock Vina and DOCK6.6 as described in the text. Docked poses are in stereo, with residues M22, Y23, H42, Q148, E152, T196, L198, F234, and W256 shown for reference. Top docking modes (highlighted) are chemically reasonable, fully contained within the binding pocket, and in agreement between AutoDock Vina and DOCK6. b) Docking

solutions of approximately the same orientation are overlaid (substrates/products are organized by left/right; docking programs AutoDock Vina/DOCK6 are organized top/bottom; force-fields UFF/MMFF94s are shown in different colors). For clarity, surrounding SpnF residues are not shown.



Supplementary Figure 7. SpnF point mutants prepared for the cyclization assay. a) Size-exclusion chromatograms and b) SDS-PAGE gel showing the well-foldedness and purity of wild-type SpnF and several point mutants.

REFERENCES

1. Kim, H.J., Pongdee, R., Wu, Q., Hong, L. & Liu, H.-w. The biosynthesis of spinosyn in *Saccharopolyspora spinosa*: synthesis of the cross-bridging precursor and identification of the function of SpnJ. *J. Am. Chem. Soc.* **129**, 14582-14584 (2007).
2. Kim, H.J., Ruszczycky, M.W., Choi, S.-h., Liu, Y.-n. & Liu, H.-w. Enzyme-catalysed [4+2] cycloaddition is a key step in the biosynthesis of spinosyn A. *Nature* **473**, 109-112 (2011).
3. Chen, Y.L., Chen, Y.H., Lin, Y.C., Tsai, K.C. & Chiu, H.T. Functional characterization and substrate specificity of spinosyn rhamnosyltransferase by in vitro reconstitution of spinosyn biosynthetic enzymes. *J Biol Chem* **284**, 7352-7363 (2009).
4. Isiorho, E., Liu, H.-w. & Keatinge-Clay, A.T. Structural studies of the spinosyn rhamnosyltransferase, SpnG. *Biochemistry* **51**, 1213-1222 (2012).
5. Kim, H.J., White-Phillip, J.A., Ogasawara, Y., Shin, N., Isiorho, E.A. & Liu, H.-w. Biosynthesis of spinosyn in *Saccharopolyspora spinosa*: synthesis of permethylated rhamnose and characterization of the functions of SpnH, SpnI, and SpnK. *J. Am. Chem. Soc.* **132**, 2901-2903 (2010).
6. Isiorho, E., Jeon, B.-S., Liu, H.-w. & Keatinge-Clay, A.T. Structural studies of the spinosyn forosaminyltransferase, SpnP. *Biochemistry* **53**, 4292-4301 (2014).